THE PENNSYLVANIA STATE UNIVERSITY
SCHREYER HONORS COLLEGE

DEPARTMENT OF MECHANICAL AND NUCLEAR ENGINEERING

PERFORMANCE OF INDUSTRIAL FLUIDLASTIC™ MOUNTS AND FEASIBILITY FOR HELICOPTER SEAT APPLICATION

ANGELA N. SANTO

Fall 2009

A thesis
submitted in partial fulfillment
of the requirements
for a baccalaureate degree
in Mechanical Engineering
with honors in Mechanical Engineering

Reviewed and approved* by the following:

Christopher D. Rahn
Professor of Mechanical Engineering
Thesis Supervisor

Mary Frecker
Professor of Mechanical Engineering
Honors Adviser

***Signatures are on file in the Schreyer Honors College.**

ABSTRACT

Negative health and performance effects are becoming increasingly important issues attributed to excessive vibrations in helicopter seats. Foam seat cushions are currently used for vibration reduction, but to further resolve these issues other methods of vibration mitigation are being explored. Fluidlastic™ technology is used in many other vibration applications due to its tunable performance at desired frequencies of operation. Industrial Fluidlastic™ mounts, designed as cab mounts in semi-trucks, provide high damping at one tunable frequency along with low damping and superior isolation at a different tuned frequency. In this thesis, the performance of industrial Fluidlastic™ mounts is compared to the performance of foam cushions currently used on helicopter seats. The results are assessed at the frequencies of interest for a Sikorsky Blackhawk helicopter, mainly four times the blade passage frequency (4/rev = 17.2 Hz). A supplemental frequency of interest is the natural frequency of the human spine (10 – 12 Hz) because excessive vibrations at this frequency could be the cause of some of the negative health effects. An experimental test stand is designed and fabricated to test the dynamic response of the mounts and the seat cushion. The test stand consists of a Ling shaker, two load cells that measure input and output force, and a LabVIEW control and data acquisition system. It is found that the mount offers a nearly 250% improvement over the cushion alone at the mount's isolation frequency, but the cushion performs better near the spinal natural frequency range. Models are developed and validated with the experimental data to determine the generalized behavior of the Fluidlastic™ mount and the cushion, and allow predictions and comparisons of performance at different preloads, internal dimensions and mount characteristics. From these models, a fluid mount redesign is proposed in order to tune the mounts to isolate vibrations at the Blackhawk 4/rev frequency and increase damping at the spinal natural frequency range. It is determined from this

research that Fluidlastic™ mounts are a viable method of helicopter seat vibration reduction and should be further investigated.

TABLE OF CONTENTS

LIST OF FIGURES

LIST OF TABLES

ACKNOWLEDGEMENTS

I would like to thank my adviser, Dr. Christopher Rahn, for helping to develop this project for me and guide my progress. Thanks are also due to Dr. Ed Smith, for all of his valuable input this semester, and also to Dr. Mary Frecker, my honors adviser, for taking the time to read my thesis. I would also like to extend my thanks to graduate student Lloyd Scarborough for his guidance, for helping me to run my experiments, and for lifting six-hundred pounds of cinderblocks on and off the test frame for each.

I also owe many thanks to LORD Corporation for their generous donation of four Fluidlastic™ mounts for me to test, and especially to Zach Fuhrer who has answered all my fluid mount questions along the way. Also, thank you to Sam Evans of the Vertical Lift Research Center of Excellence for procuring a foam seat cushion.

Finally, thanks to my family and friends for keeping me motivated along the way. Dad, Mom, Kelly and Chris – my goal is always to make you proud.

1. INTRODUCTION

Helicopters are some of the most delicate vehicles to fly due to resonant conditions occurring at the main and tail rotor rotational frequencies as well as their harmonics. Because of the high sensitivity to motion, vibration and motion control products have been developed for engines, rotor blades, pitch links and a variety of other helicopter components, including pilot and co-pilot seats. Cockpit seats currently utilize specially designed foam cushions to control vibration transmissibility from the floor through the seat to the seated individual. Figure 1 shows an example of the current seating setup in a helicopter cockpit. The effectiveness of foam cushions is questionable, however. Previous studies and surveys involving helicopter aircrew members have determined there is a relatively high incidence of negative health effects attributed to extended periods of sitting in the cockpit. Studies have also been completed exploring the performance and feasibility of other vibration reduction methods for a helicopter seat.

Figure 1: Sikorsky Vibration Simulation Seat with Sikorsky Blackhawk Back and Bottom Seat Cushions

1.1. WHOLE-BODY VIBRATION EFFECTS

Whole-body vibration (WBV) occurs when a person’s body weight is being supported by a vibrating surface, and operators of trucks, tractors, trains, fixed-wing aircraft, rotary-wing aircraft, and countless other vehicles are exposed to WBV on a daily basis [1]. WBV has become a major concern for helicopter pilots because it can accelerate fatigue, therefore decreasing mission efficiency and effectiveness, and it can cause permanent injury to the lower back [1]. Lumbar syndrome is the most common affliction reported by those exposed to whole-body vibration; it encompasses any disorders related to degeneration of disks in the lower back [2]. In a survey of over 100 helicopter pilots, 87.5% reported back pain while cervical and thoracic pain were also reported [3; 1]. According to a 1984 study conducted by Froom, *et al.* the occurrence of vertebrae slippage in the lower back region of the spine is 4.5 times more common in helicopter pilots than cadets who have not flown an aircraft [4]. This type of slippage is caused by repeated back extension [5], which could be attributed to the constant vibration force experienced by the pilots. Average onset time of pain and numbness in the back and legs is between 2 and 4 hours of flight [6; 7], and depending on the total flight time exposure this pain can become chronic [7]. In addition to the prevalence of pain and injury, seat cushions were previously found to be insufficient in isolating the effects of whole-body vibration. Paddan and Griffin found that seating isolation efficiency in helicopters was 251.1%, where values less than 100% corresponded to some decrease in vibration [8]. The following section discusses methods, other than foam cushions, of damping and isolating seat vibrations that have already been investigated.

1.2. VIBRATION REDUCTION APPROACHES

Helicopter seats currently utilize foam cushions which are placed between the seat frame and the occupant's body, providing passive damping and very little vibration isolation. Another passive device which has been studied is a dynamic anti-resonant vibration isolator (DAVI). A DAVI is composed of a spring system and a moving mass installed between the vibrating structure and the isolated structure [9]. The moving mass provides vibration attenuation over a range of frequencies as well as zero vibration at a single, tunable frequency [9]. In 2008, a group of Penn State students installed a DAVI under a helicopter simulation seat and found that it reduced vibration levels by 95% at the blade passage frequency of a Sikorsky Blackhawk helicopter [10]. DAVIs are a viable option for this application because the moving mass can be adjusted to isolate any frequency, but a typical DAVI does not provide any damping at the natural frequency of the system.

Research has been completed regarding active and semi-active vibration control of helicopter seat vibrations as well. In 2008, Chen, *et al.* developed a proof-of-concept model for an adaptive control system which utilizes a miniature modal shaker as the actuator mechanism [11]. This adaptive control system is able to adjust to changing flight conditions, such as vibration frequencies and aircrew member weight and posture, so it provides much better vibration reduction than a passive seat cushion alone [11]. It was determined that the combination of the cushion and the adaptive control reduced vibrations in the vertical direction by approximately 50% at the blade passage frequency, and vibration levels at other frequencies of interest saw either no change or an improvement [11]. Magneto-rheological dampers are a semi-active solution that has also been tested for feasibility in a helicopter seat application. Like the adaptive control system, the damping ratio in magneto-rheological dampers can be adjusted at all times to account for changing flight conditions [12]. It was found that magneto-rheological dampers caused a 61-70% improvement in seat vibrations at the blade passage frequency [12]. This allows for high damping at the natural frequency of the system and low damping over the remainder of the frequency range, which permits better vibration isolation at the blade passage frequency.

1.3. FLUIDLASTIC™ DEVICES

Fluidlastic™ devices utilize both rubber and fluid to provide passive vibration damping and isolation. The fluid flow provides high damping at a tuned frequency and low damping elsewhere in the frequency range; it also completely isolates vibrations at a separate specified frequency [13]. The rubber section is responsible for the stiffness characteristics which limit basic motions [13]. Fluidlastic™ devices are passive like DAVIs; the only difference is that the solid moving mass is replaced by fluid flow in a Fluidlastic™ mount.

Fluidlastic™ technology was first developed by LORD Corporation and was originally used to damp and isolate vibrations in engines [14]. Today its range of uses has expanded to include aerospace, industrial transportation, and wind energy applications [15]. More complex Fluidlastic™ devices are already present on helicopter rotors, and installing industrial fluid mounts on pilot and co-pilot seats could be the next step. Fluidlastic™ devices are lightweight, statically stiff and dynamically softer, maintenance-free, and tunable to fit the desired application [13]. These attributes are all desirable for helicopter applications.

1.4. RESEARCH OBJECTIVES

The main objective of this research is to compare the performance of industrial fluid mounts to foam seat cushions in their ability to reduce vibrations transmitted from the helicopter floor to aircrew members through the seat. A supplemental objective is to design, build and implement experiments to determine the behavior of LORD Corporation Fluidlastic™ mounts and Sikorsky UH-60 Blackhawk seat cushions. From the experimental results, derive two models that represent the behavior of the mount and the cushion, respectively. Subsequently, adjust model parameters for the mount in order to obtain an optimal design, which would isolate vibrations at the desired frequency. Finally, combine experimental results with previous research and generalized cockpit size and weight limitations to determine the feasibility of utilizing Fluidlastic™ mounts in a helicopter seat application.

2. MATERIALS AND METHODS

2.1. LORD CORPORATION FLUIDLASTIC™ MOUNT

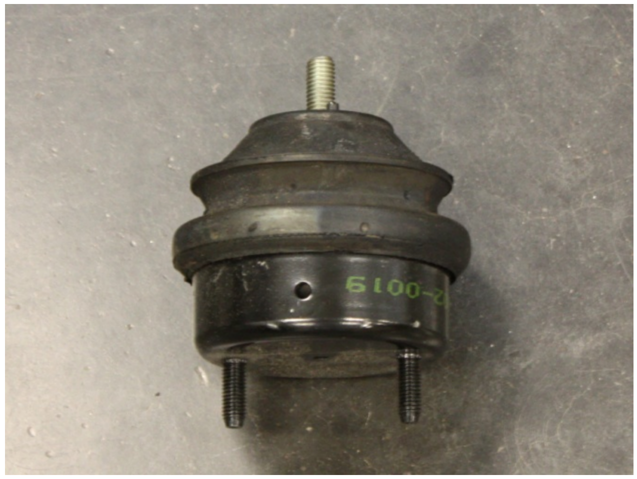

Figure 2: LORD Corporation Fluidlastic™ Mount, J-18569-Series

The mounts undergoing evaluation for this experiment are LORD Corporation Fluidlastic™ mounts, shown in Figure 2, which can be viewed in LORD's online Industrial Applications catalog [13]. These particular mounts are part of the J-18569 product line, which offers an array of rubber and fluid mounts with different frequencies of maximum damping. The mounts are composed of low carbon steel, aluminum alloy, black rubber and fluid. The fluid is a LORD Corporation proprietary product specially designed with a certain density and viscosity based on design frequencies as well as the environmental conditions of the application. The rubber is a LORD Corporation proprietary black rubber blend which is bonded to the inner member using a LORD Corporation specialty adhesive. In general, these mounts, like all rubber parts, are meant to be loaded in compression then exposed to a dynamic force or displacement. Black rubber is a very strong material in compression, but very weak in tension, which is why most rubber parts, including this mount, are pre-compressed to some degree prior to use. As an additional measure to prevent tensile loading, the inner member and rubber section is unable to extend beyond a certain point due to stops in place on the inner diameter of the housing.

Most of the fluid mount's performance characteristics are determined by the internal geometry and flow process. Externally, the black rubber section acts as a spring, providing the basic load-bearing and motion-restricting capabilities. Sealed inside the metal and rubber shell is a LORD Corporation proprietary fluid which flows between two chambers via an inertia track and a damping element. The fluid flow allows for excellent vibration isolation at a single frequency which is independent of any preload conditions. The isolation frequency depends on various internal mount characteristics such as inertia track dimensions and fluid density. The fluid also flows through a damping element which provides high damping at a tunable frequency. The basic internal geometry is shown in Figure 3.

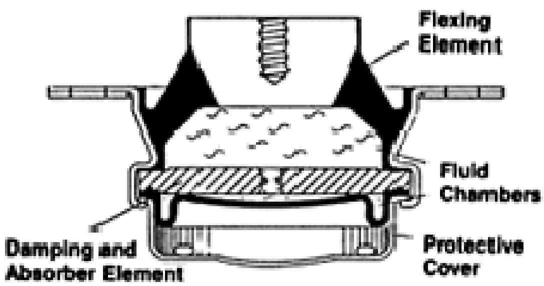

Figure 3: Fluid Mount Schematic [15]

When a displacement is applied to the inner member, the rubber section flexes and reduces the volume of the upper chamber. Some of the fluid flows through the specially designed inertia track into the lower chamber, and the rest of the fluid flows through the damping element. Whereas the upper chamber has essentially rigid walls, the bottom chamber acts as a fluid capacitor with flexible rubber walls, allowing the volume of the lower chamber to change with time. On the upward stroke of dynamic displacement, the spring rate of the lower chamber wall provides enough force to move fluid back through the inertial track and damping element into the upper chamber, where the fluid flow process begins again.

This type of mount is used most commonly as a cab mount on a semi-truck to reduce the effect of ground vibrations, but it is also used in other industrial applications such as engine-generators [13]. These particular mounts are tuned to provide exceptional damping at a frequency of 6 Hz within a preload range of 200 – 400 pounds. The frequency of isolation is not listed on the part drawing; it will be determined experimentally.

2.2. SIKORSKY UH-60 BLACKHAWK SEAT CUSHION

Figure 4: Bottom Section of Sikorsky Blackhawk Seat Cushion

The UH-60 Blackhawk cushions come as a set which includes a bottom cushion and a backrest cushion. The main focus of this experiment is to test the vibration reduction in the vertical direction, therefore only the bottom seat cushion is used. The bottom cushion consists of three layers of different density foams encased in a removable fabric shell. Figure 4 shows an isometric view of the cushion. Refer to Figure 1 in the Introduction to see the application of the full cushion set on an actual helicopter seat. The cushion composition is as follows: the bottom layer is relatively stiff foam, the middle layer is presumably softer, energy-absorbing foam, and the top layer is most likely polyurethane foam. These assumptions are based on a description of similar AH-64 Apache seat cushions in Suzanne D. Smith's research of prototype cushions [16]. The cushion is contoured to fit the human body, but for testing purposes, an approximately rectangular section is removed from the center of the bottom cushion. This enables the mount and the cushion to be tested identically on the same test stand. The dimensions of the cushion section, shown in Figure 5, are approximately 9" x 6" x 3".

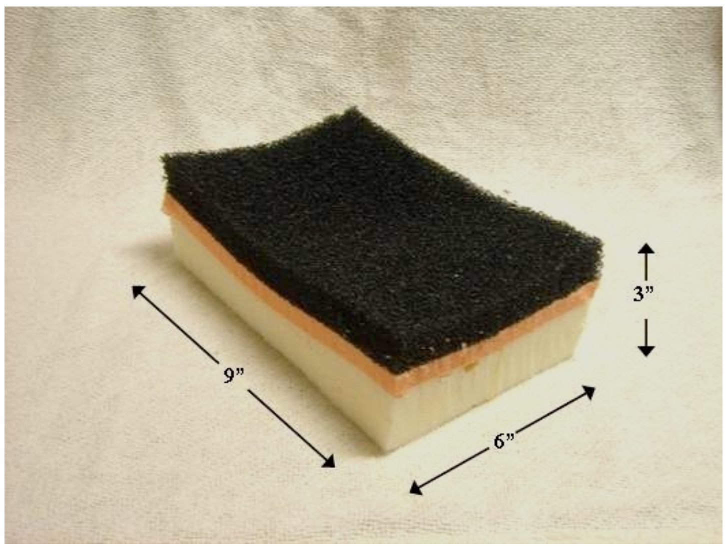

Figure 5: Rectangular Cushion Section for Experimentation Purposes

2.3. TEST SETUP AND EQUIPMENT

Figure 6 shows the basic setup of the fluid mount testing system. The testing utilizes a simple aluminum test frame placed directly on a concrete floor. Two aluminum bars span the width of the frame and represent ground. The right-hand side of ground has a $50\, lb_f/mV$ piezoelectric force sensor (PCB Piezotronics, Model 208C02) installed between it and the test specimen. The left-hand side of ground has a quarter-inch threaded stud to account for the height difference. Two sections of angle iron surround the force sensor and threaded stud to increase support and protect the force sensor from damage. The mount is bolted directly to the top angle iron section via the two M10 x 1.5 mm studs on the housing using two M10 x 1.5 mm flange nuts. Finally, the load frame bolts onto the mount via the M12 x 1.75 mm stud protruding from the top surface of the mount, using an M12 x 1.75 mm flange nut to secure the frame in place. The load frame consists of two loading plates connected by four sections of angle iron, forming a trapezoidal shape. Having two loading plates maximizes the area where load can be applied and also allows for the system to be excited from the floor below. The bottom load plate connects to another $50\ lb_f/mV$ piezoelectric force sensor which leads to a modal shaker (Ling LMT-100).

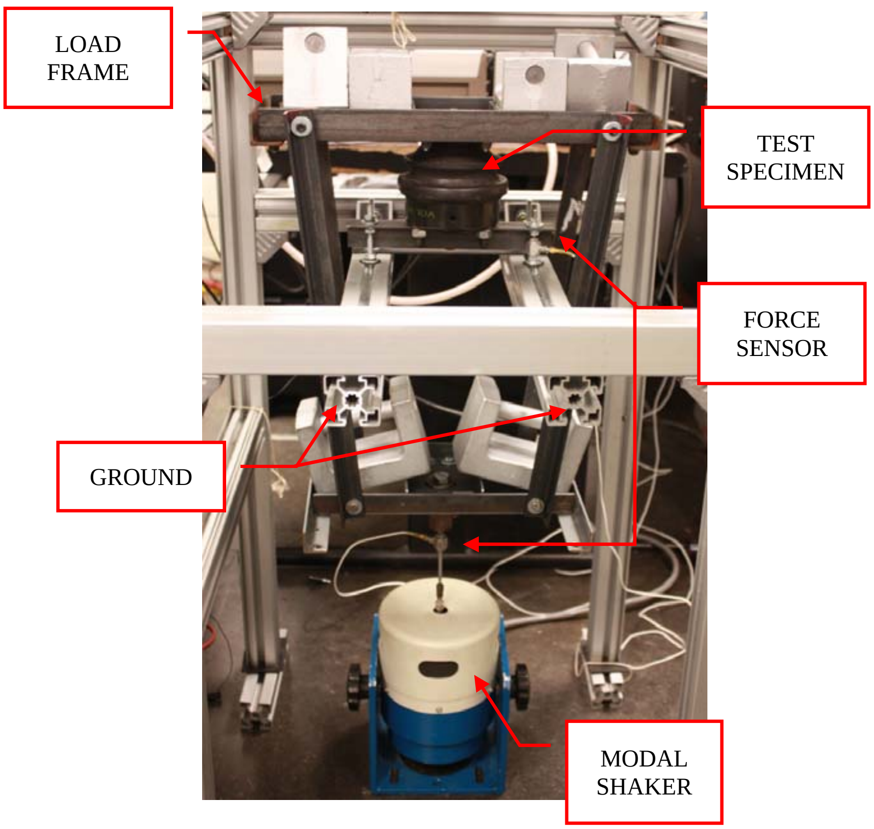

Figure 6: Basic Test Frame Setup

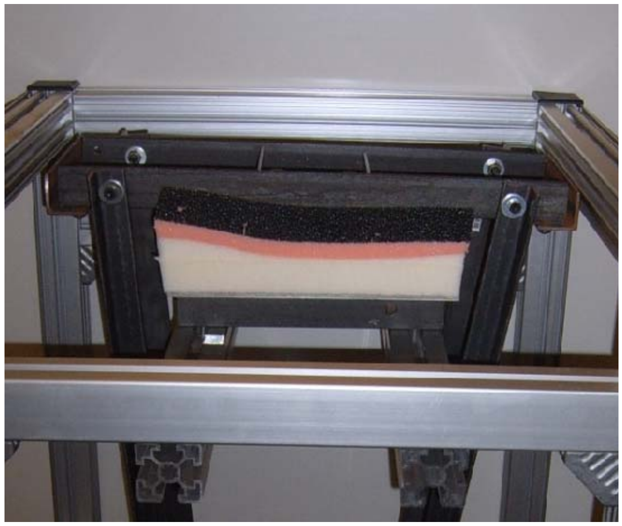

Figure 7: Test Setup Using Seat Cushion Section

The seat cushion is placed on the test frame in a slightly different fashion from the mount, and this is pictured in Figure 7. An aluminum plate is cut to the length and width dimensions of the cushion, and it has two holes cut to the dimensions of the threaded studs protruding from ground (these can also be seen in Figure 6). The plate rests on the top angle iron section and is attached to ground via the two threaded studs. The cushion sits between the load frame and the aluminum plate but is not physically attached to either.

A LabVIEW program inputs an arbitrary amplitude sinusoidal signal which sweeps across the 0 to 60 Hz frequency range over a period of 30 seconds. The signal is fed through an amplifier (STAR Amplifier, compatible with Ling LMT-100 shaker) and into the modal shaker. Once the vibrations are transmitted through the test specimen, the force sensor at ground sends an output signal to LabVIEW. The signal is sent through a high-pass filter with a cutoff frequency of 60 Hz and averaged five times to refine the output. LabVIEW outputs the ratio of force from the shaker to one-half of the force felt by ground. Experimental results are multiplied by two to account for the division of ground into two sides.

2.4. TESTING

Two identical mounts were used for testing, which are referred to herein as Mount #1 and Mount #2. For each mount and the single section of cushion, three different preloads are applied (P_1 = 209.5 lb_f, P_2= 229.5 lb_f, and P_3 = 249.5 lb_f). The preloads are achieved by loading the load frame with a combination of 4” x 8” x 16” concrete blocks and calibrated laboratory weights, along with the weight of the test frame. The average weight of a concrete block is 32.5 lb_f, and the load frame weighs 14.6 lb_f.

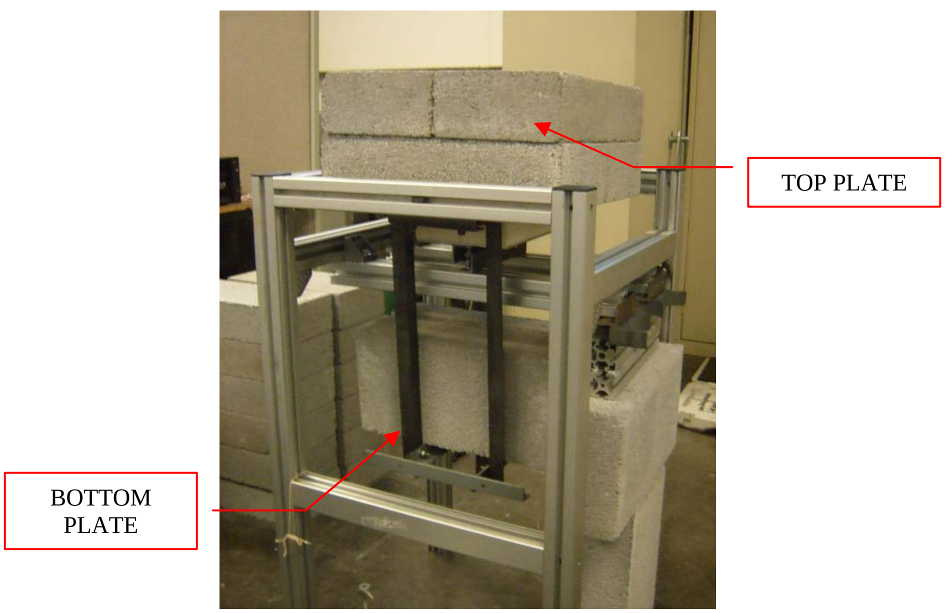

Figure 8: Preload Distribution on Load Frame

The preload is distributed on the load frame as shown in Figure 8. Four concrete blocks (as well as any supplemental calibrated weights) are balanced on the top plate of the load frame. Two concrete blocks sit on the bottom plate of the load frame, helping to balance the slightly top-heavy frame.

Figure 9: Loading of Aluminum Test Frame

Twelve concrete blocks are placed on the aluminum test frame so that it is approximately twice as heavy as the system being excited. The loaded-down frame is shown in Figure 9. None of the concrete blocks placed on the aluminum test frame interfere with the motion of the load frame.

3. RESULTS

3.1. FLUID MOUNT MODELING

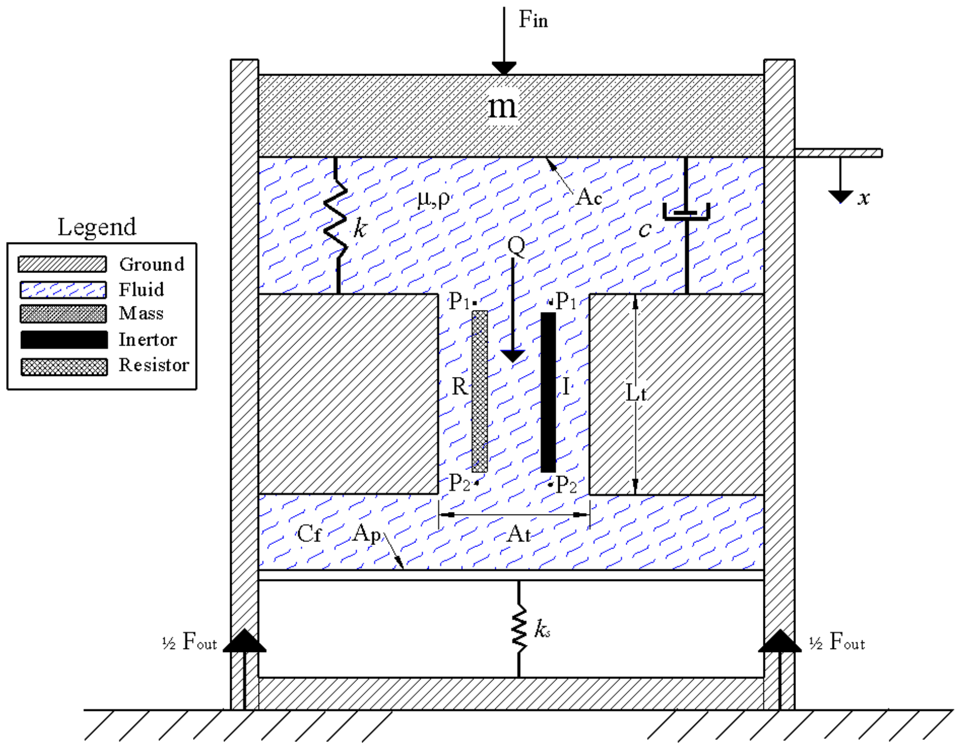

Figure 10: Fluid Mount Simplified Model

The mount is modeled as a fluid-mechanical device as shown in Figure 7. From the free-body diagram of the mass we obtain

$$m\ddot{x} + c\dot{x} + kx = F_{in} - P_1 A_c, \quad (1)$$

where m = mass, c = viscous damping constant, k = spring constant, A_c = piston area, x(t) = displacement at the mass, F_{in}(t) = input force and P_1(t) = pressure in upper fluid chamber. Using the compatibility equation for the inertia track yields the equation

$$P_1 - P_2 = I\dot{Q} + RQ, \quad (2)$$

where I = inertance of fluid, R = fluid resistance of inertia track, P_2(t) = pressure in lower fluid chamber, and Q(t) = flow rate. The elemental equation for a fluid capacitor yields

$$Q = C_f \dot{P}_2, \tag{3}$$

where C_f = capacitance of lower fluid chamber. The fluid-mechanical coupling equation is

$$Q = -\rho A_c, \tag{4}$$

where ρ = fluid density. Finally, from the free body diagram of the housing we obtain

$$0 = P_1(A_c - A_t) + F_{out} + P_2 A_t - kx, \tag{5}$$

where A_t = area of inertia track and F_{out}(t) = output force to ground. Taking the Laplace transform of equations (1) through (5) allows us to solve the system and we obtain the force transfer function

$$T_{mount} = \frac{F_{out}}{F_{in}} = \frac{\left[(A_c - A_t)IC_f\right]s^2 + \left[(A_c - A_t)RC_f\right]s + A_c + \dfrac{kC_f}{\rho A_c}}{\left(IC_f + \dfrac{mC_f}{\rho A_c}\right)s^2 + \left(RC_f + \dfrac{cC_f}{\rho A_c}\right)s + \dfrac{kC_f}{\rho A_c} + 1}. \tag{6}$$

3.1.1. FLUID MOUNT MODELING PARAMETERS

Modeling parameters are determined using a combination of drawing specifications, part dimensions, experimentation, and estimation. The spring constant (*k*) is the static stiffness of the part as listed on the drawing, and the damping constant (*c*) is determined using

$$c = \eta\sqrt{km}, \tag{7}$$

where the assumed loss factor is $\eta = 0.07$. Damping ratios for black rubber types are typically between 0.05 and 0.1. The total applied load to the system (*m)* is determined by dividing the applied load, P_n *(n* = 1, 2, or 3), by the acceleration due to gravity, $g = 386.4 \, {}^{in}/_{s^2}$. We experimentally determine the average fluid density (ρ) by weighing various fluid samples on a triple-beam balance.

We model the inertia track to have both a fluid inertance (I) and a fluid resistance (R). The track is approximated as circular with a non-uniform, parabolic velocity profile, so we obtain the inertance to be

$$I = \frac{2\rho A_t}{L_t}, \tag{8}$$

where L_t = inertia track length. Assuming the same inertia track characteristics we obtain

$$R = \frac{128\mu L_t}{\pi d^4} \tag{9}$$

as the fluid resistance, where μ = fluid viscosity and d = inertia track diameter. All inertia track dimensions are proprietary to LORD Corporation. We estimate the fluid viscosity by comparing the fluid's density, appearance, and scent to other known fluids. The inertia track diameter is approximated using

$$d = \sqrt{\frac{A_t}{\pi}}. \tag{10}$$

Finally, the bottom fluid chamber is modeled as a fluid capacitor, consisting of a piston whose force is counteracted by a spring. The fluid capacitance for this type of capacitor is

$$C_f = \frac{{A_p}^2}{k_s}, \tag{11}$$

where A_p = piston area and k_s = spring stiffness. The piston area is assumed to be equal to the inertia track area, A_t. The spring stiffness is adjusted until the natural frequency peak of the model matches the experimental peak. The total force exerted by the fluid on the chamber walls divided by the chosen spring constant yields a reasonable displacement for the piston, justifying our choice for k_s. The final model parameter we determine is the piston area, A_c, of the mount. The area is adjusted until the isolation frequency of the model matches the experimental results. The value of A_c is within the dimensional constraints listed on the part drawing.

3.1.2. FLUID MOUNT RESULTS

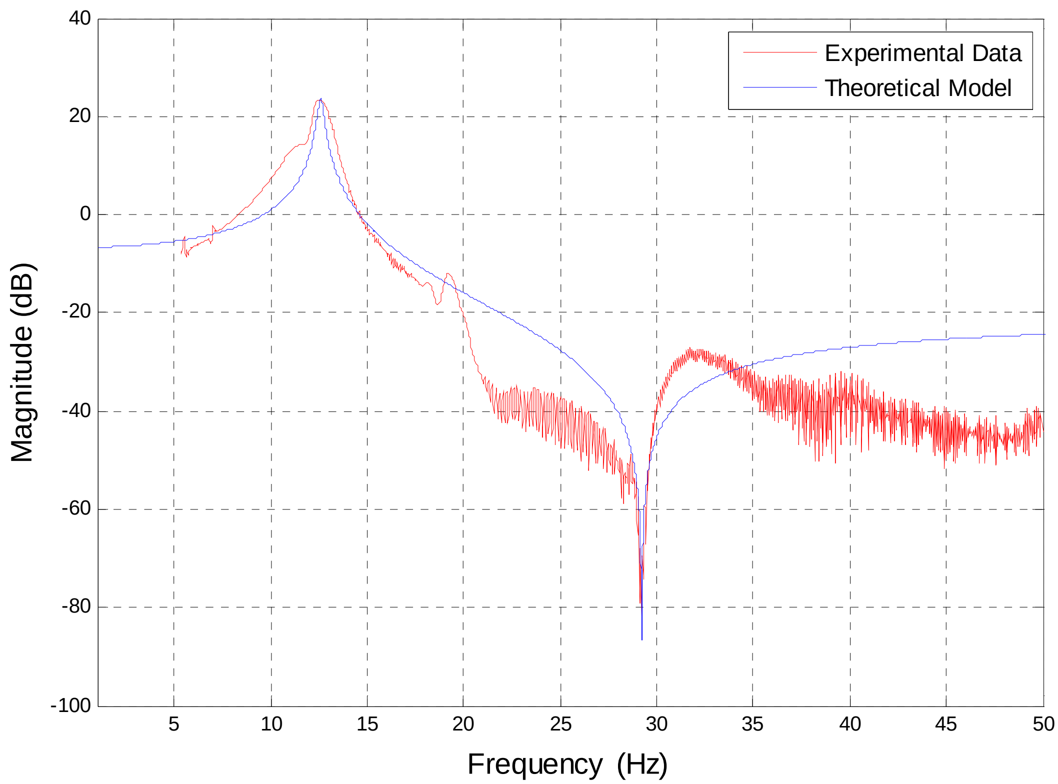

Figure 11: Theoretical and Experimental Frequency Response of Fluid Mount #1 (P = 209.5 lb_f)

We generate a bode plot in MATLAB for the transfer function T_{mount} using the parameters determined in section 3.1.1, which is represented by the solid blue line in Figure 11. The experimental results are shown in red. Figures 19 and 20 in Appendix A show plots for the remainder of the tests performed on Mount #1.

There is a distinct natural frequency peak and a distinct isolation frequency in the model, which matches the general trend of the experimental data.

		Isolation Frequency (Hz)			Magnitude (dB)		
		Experimental	**Theoretical**	**% Error**	**Experimental**	**Theoretical**	**% Error**
Mount #1	$\mathbf{P_1}$	29.2	29.2	0.0	-83.5	-86.8	-3.8
	$\mathbf{P_2}$	29.2	29.2	0.0	-98.9	-87.4	13.2
	$\mathbf{P_3}$	28.4	29.2	-2.8	-68.9	-88.0	-21.7

Table 1: Comparison of Theoretical and Experimental Results for Isolation Frequency, Mount #1

		Natural Frequency (Hz)			Magnitude (dB)		
		Experimental	**Theoretical**	**% Error**	**Experimental**	**Theoretical**	**% Error**
Mount #1	$\mathbf{P_1}$	12.5	12.6	-0.8	23.5	23.6	0.0
	$\mathbf{P_2}$	12.1	12.2	-0.8	23.6	23.5	0.4
	$\mathbf{P_3}$	11.4	11.9	-4.2	17.7	23.4	-24.4

Table 2: Comparison of Theoretical and Experimental Results for Natural Frequency, Mount #1

The theoretical and experimental results for isolation frequency are shown in Table 1, and a similar comparison of natural frequencies is shown in Table 2. The maximum error for the isolation frequency is 2.8%, while it is slightly higher at 4.2% for the natural frequency. This can most likely be attributed to the loading method, which causes slight imbalances and, therefore, additional natural frequencies. The comparison of magnitudes becomes progressively worse as loading increases, which can also be attributed to the loading method.

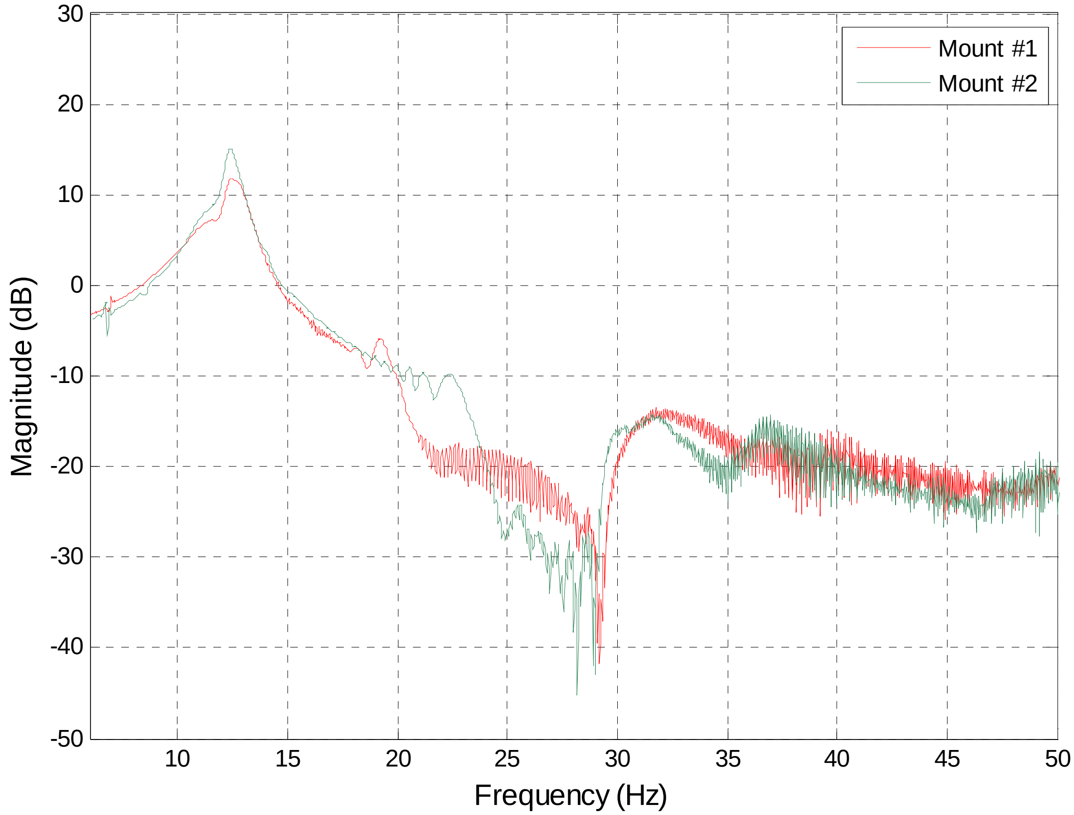

Figure 12: Fluid Mount Transmissibility Comparison with 209.5 lb_f Load

The testing of Mount #2 yielded similar results to Mount #1, as can be seen in Figure 12, but there are additional natural frequencies at or near the isolation frequency causing higher magnitude noise between 25 and 30 Hz. This discrepancy is caused by slight differences in the balance of the load frame for the two tests. The closest experimental zero frequency to the theoretical 29.2 Hz was used for comparison and % error calculations. The maximum error for the isolation frequency of Mount #2 is also 2.8 %, and the error for the natural frequency is again slightly higher at 6.2%. We determined from the testing of Mount #2 that our testing is not mount-dependent and similar results can be achieved using any mount.

3.2. FOAM CUSHION MODELING

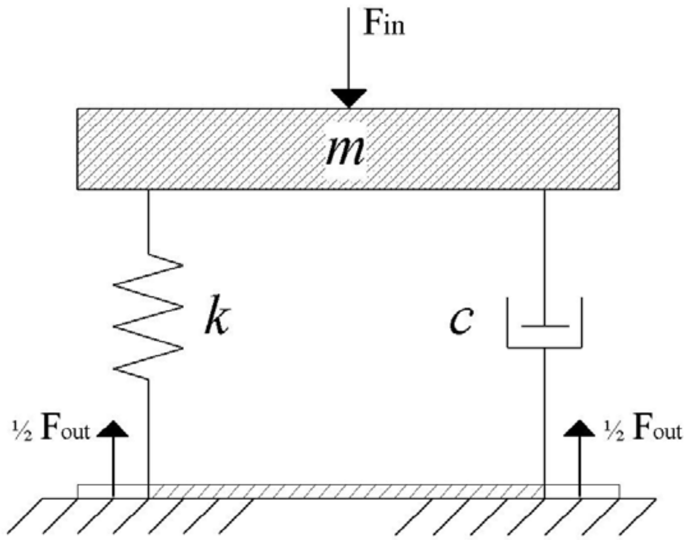

Figure 13: Seat Cushion Model

The cushion is modeled as a mass-spring-damper system, with an equivalent stiffness, *k,* representing the different stiffness values of the cushion layers. From the free body diagram of the mass we obtain

$$m\ddot{x} + c\dot{x} + kx = F_{in} \tag{12}$$

where m = mass, c = viscous damping constant, k = spring constant and F_{in}(t) = input force. The free body diagram of the ground yields

$$0 = F_{out} - c\dot{x} - kx, \tag{13}$$

where F_{out}(t) = output force. After taking the Laplace transform of each equation and solving equations (7) and (8) for the force transfer function, we obtain

$$T_{cushion} = \frac{F_{out}}{F_{in}} = \frac{cs + k}{ms^2 + cs + k}. \tag{14}$$

3.2.1. CUSHION MODELING PARAMETERS

Modeling parameters are determined using the natural frequency of the experimental data and the assumption that the cushion has a loss factor of η = 0.13. We obtain the spring constant using

$$k = m\omega_n{}^2, \tag{15}$$

and we obtain the damping constant, c, using Equation 7 from section 3.1.1.

3.2.2. CUSHION RESULTS

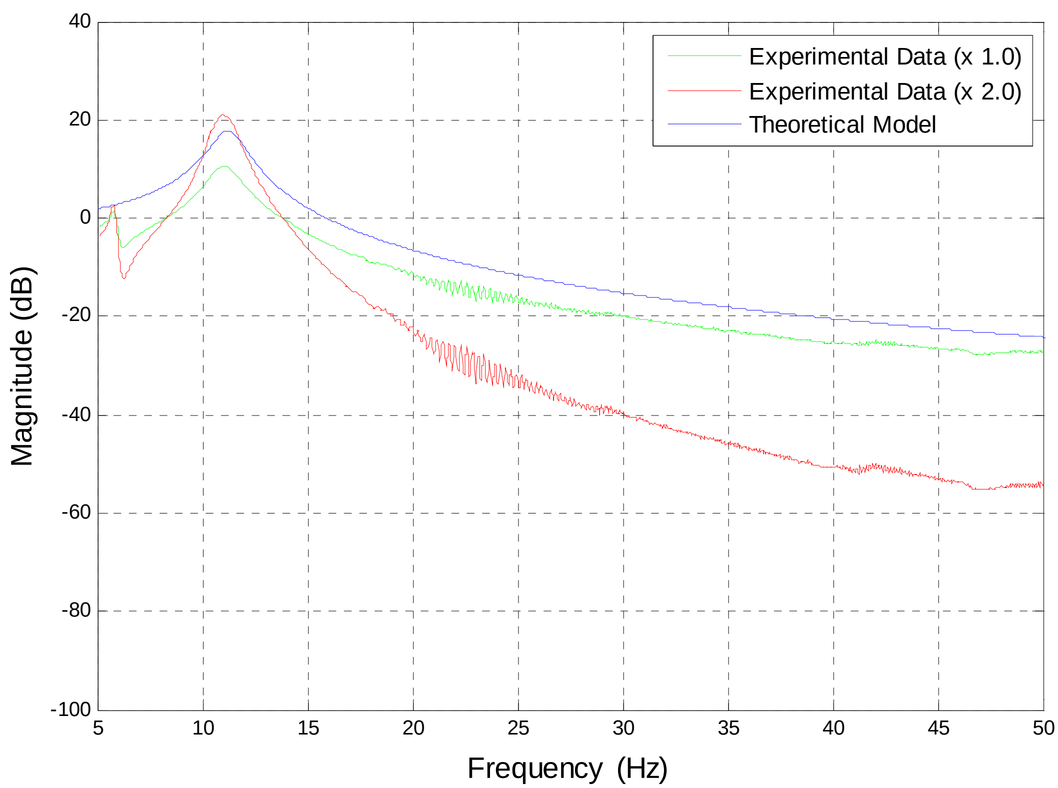

Figure 14: Theoretical and Experimental Frequency Response of Foam Cushion (P = 209.5 lb$_f$)

Generating a bode plot in MATLAB for the transfer function $T_{cushion}$ using the parameters determined in section 3.2.1 yields the results represented by the solid blue line in Figure 14. The behavior of the foam cushion is not as simple as that of the fluid mount, however. When the experimental data is multiplied by two (as discussed in Section 2.3), the result is shown by the red line in Figure 14. However, if the experimental data is not subject to a multiplication factor, the result is represented by the green line. The model follows the trend of the unaltered experimental data much more closely than the trend of the data multiplied by two. This comparison shows that the load is most likely not divided evenly between the two ground locations. An explanation for this is that slightly uneven cushion dimensions leads to varied stiffness over the volume of the cushion. To account for the offset between the model and experimental results, a factor of 0.5 is applied to the model; these results are shown in Figure 15.

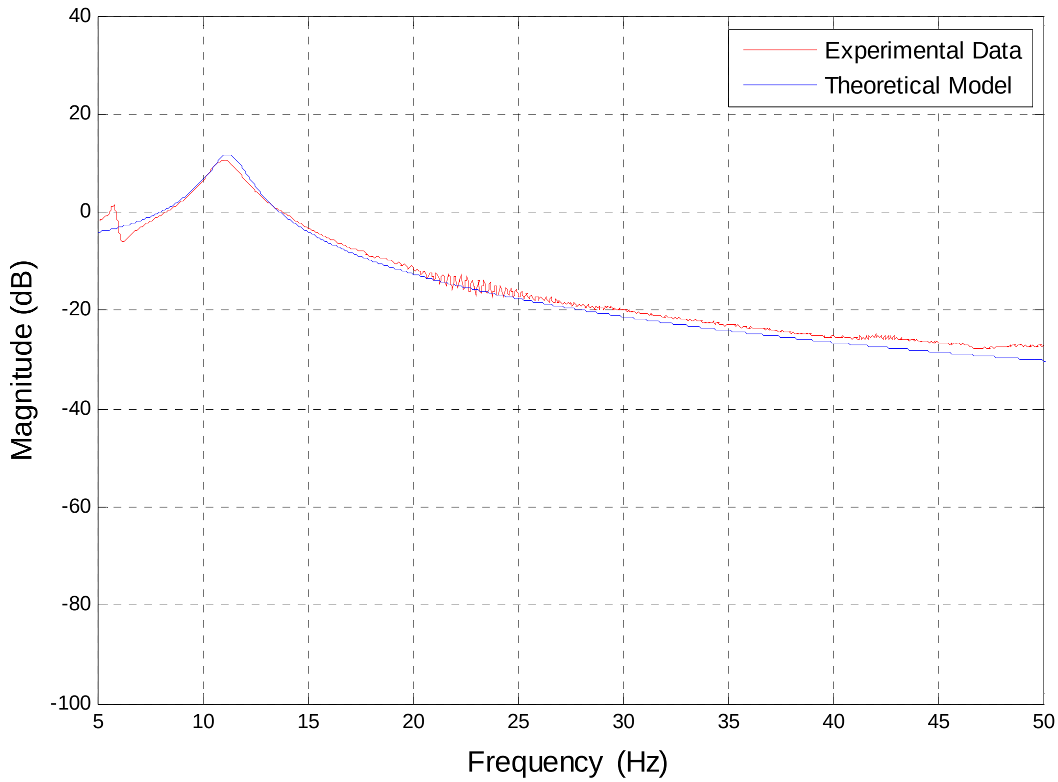

Figure 15: Experimental and Adjusted Theoretical Foam Cushion Results (P = 209.5 lb$_f$)

In order to use this model for analysis, it is very important to apply the correction factor to the model so that the rates of decay match and the cushion can be accurately compared to the fluid mount. Figures 21 and 22 in Appendix A show plots for the remainder of the tests performed on the cushion.

3.3. MOUNT AND CUSHION COMPARISON

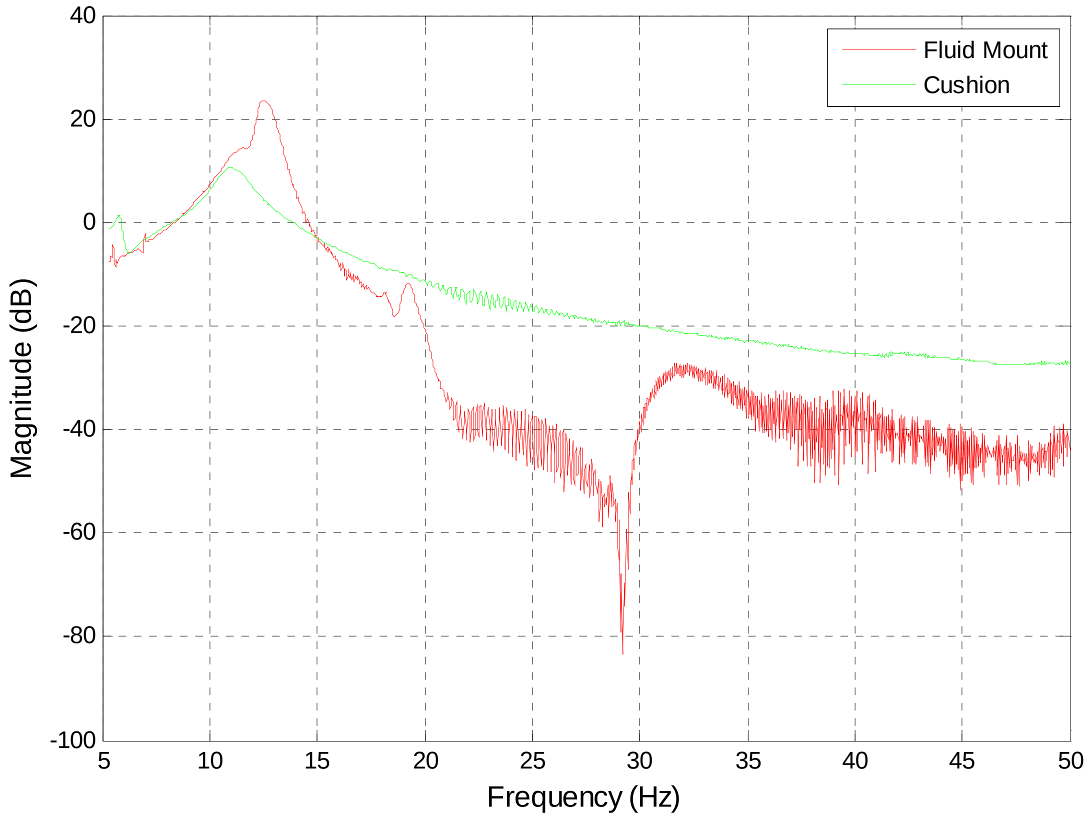

Figure 16: Comparison of Force Transmissibility for Fluid Mount and Blackhawk Seat Cushion

As can be seen in Figure 16, the cushion provides approximately twice as much damping around the natural frequency of the system than the fluid mount. However, the natural frequency of the system with the cushion is 10.9 Hz, which is within the 10-12 Hz range of natural frequencies for a human spine (6). The natural frequency of the system with the mount is just outside this range at 12.6 Hz. Over the 22 – 30 Hz range, the fluid mount provides an average improvement in vibration attenuation of about 100%, with a maximum improvement of nearly 250% occurring at the isolation frequency (29.2 Hz). Over the remainder of the frequency range, the fluid mount provides an approximate improvement of 50%. Figure 17 shows the percent improvement in vibration attenuation offered by the mount over the entire frequency range.

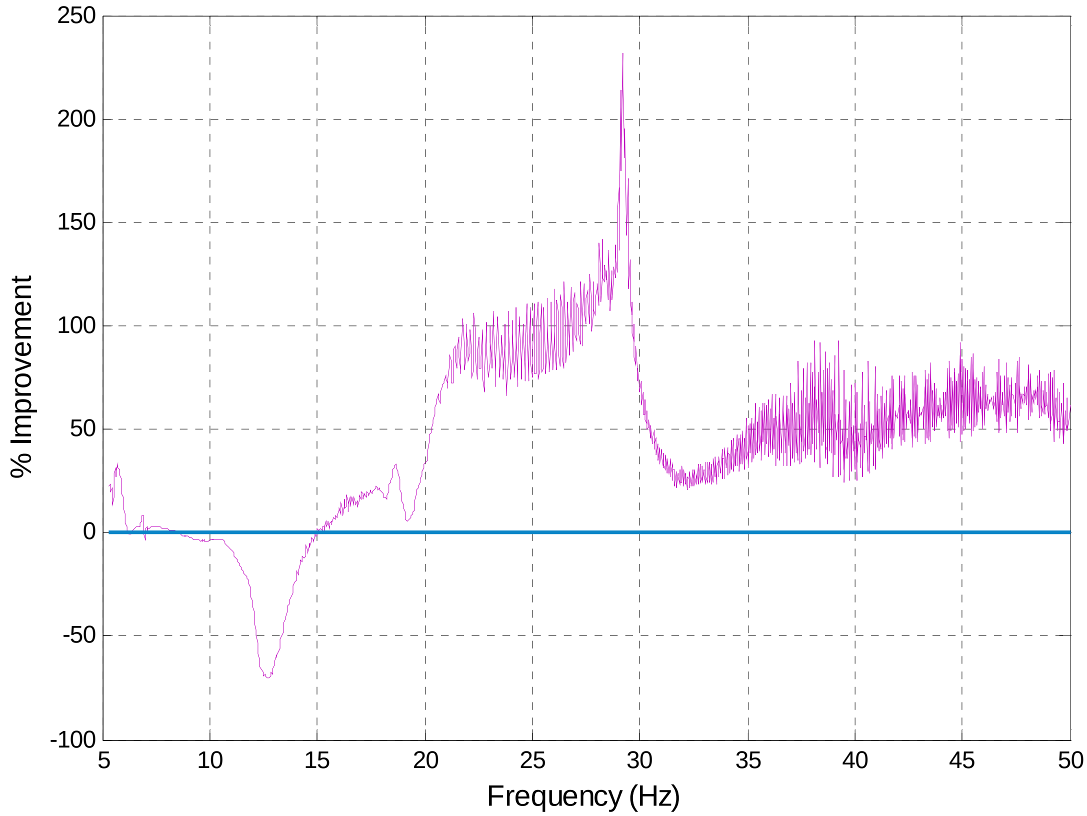

Figure 17: Percent Improvement Offered by Fluid Mount over Cushion

The only region where the mount does not offer an improvement over the cushion is near the natural frequency of the system. This is expected since the mount being tested is tuned to have maximum damping at 6 Hz and the natural frequency of the system is approximately double that. Modifications of the tuned damping frequency as well as alterations to other mount characteristics and dimensions are discussed in the next chapter.

4. CONCLUSION

4.1. DISCUSSION OF FEASIBILITY

The modeling results in Chapter 3 show the models are a valid means to locate the natural and isolation frequencies of both the cushion and the fluid mount. Some nuances exist which cannot be modeled using the simple transfer functions derived, but the models do provide enough information regarding the general behavior to allow us to use the models for further analysis.

Fluid mounts would undoubtedly add some weight to the cockpit and possibly affect the balance of the helicopter in flight, but in comparison to the active and semi-active solutions discussed in Chapter 1, the fluid mounts are relatively light. The trade-off is the active and semi-active systems can be tuned during a flight whereas the fluid mounts cannot. Fluid mounts do provide a mass-independent isolation frequency, however, so the absence of the adjustment capability based on individual pilot weights is inconsequential. Additionally, the fluid mounts provide a more compact solution than the DAVI, the other passive solution from Chapter 1, by replacing the solid moving mass with a lightweight fluid to achieve a tuned isolation frequency. Installation of fluid mounts onto a helicopter seat will require minimal modifications to the existing system due to the small size (approximately 4.75” diameter and 3.5” height) and readily accessible threaded connections.

A helicopter cockpit is affected primarily by the main rotor blade passage frequency, particularly the 4^{th} harmonic, abbreviated 4/rev. On most helicopters, the 4/rev frequency is in the 20 – 30 Hz range [17], and the Sikorsky UH-60 Blackhawk has a 4/rev of 17.2 Hz [18]. This particular fluid mount provides an insignificant improvement over the Blackhawk seat cushion at 17.2 Hz, but it does provide a considerable improvement over the typical 4/rev range of 20 – 30 Hz. These mounts are tunable to a particular isolation frequency, however, by changing some internal dimensions as well as modifying the fluid properties, so they can be redesigned for use on a Sikorsky UH-60 Blackhawk. Assuming that four mounts are installed on a seat for balance, specifics of this proposed redesign are shown in Figure 18.

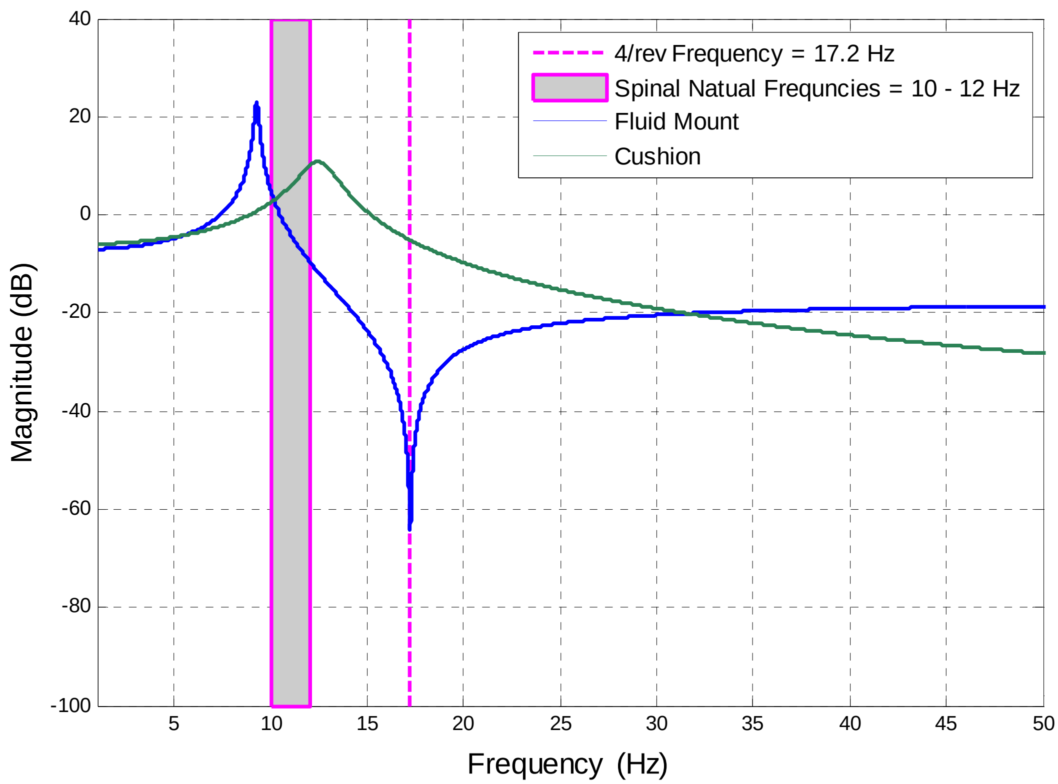

Figure 18: Mount Redesign for Use on Sikorsky UH-60 Blackhawk Helicopter Seats

The inertia track length (L_t) is increased by 10% while the inertia track area (A_t) and fluid density (ρ) are decreased by 10%. The piston area (A_c) is reduced by 20%, and finally, the two spring constants, k and k_s, are decreased by 75%. This large decrease in the stiffness is necessary because installing four mounts reduces the preload to a quarter of the original value. Using these parameters in the transfer function T_{mount}, the value of the isolation frequency is now equal to the 4/rev frequency of a Sikorsky Blackhawk helicopter. The natural frequency is also below the resonant frequency range of the spine for a large range of pilots, from a 25^{th} percentile young female to a 75^{th} percentile older male. Figure 18 shows the mount behavior assuming a 120-pound, 25^{th} percentile female pilot, and adding additional weight will simply cause the natural frequency to decrease. While this research only studies the feasibility of these mounts on a Blackhawk helicopter, the same type of modifications can be applied to isolate the 4/rev frequency of virtually any helicopter on the market. Additionally, there is no indication that the addition of a fluid mount in series with the current seat cushion will cause vibration levels to worsen.

Based on the research and analysis conducted here, the fluid mount looks to be a viable solution to reduce vibration levels in helicopter cockpit seats. Section 4.2 discusses future research and recommendations to further judge the feasibility of one day installing fluid mounts underneath a helicopter seat.

4.2. RECOMMENDATIONS FOR FUTURE RESEARCH

The current model does not incorporate the tunable frequency for maximum damping because the 6 Hz frequency was too low to be detected from these tests. For another possible redesign of the mount, the maximum damping frequency can be tuned to be somewhere in the range of spinal resonances where we are currently seeing the system natural frequency. All redesigning will require consultation with LORD Engineers to determine whether a current Fluidlastic™ mount in production will fit the desired characteristics, or if a new mount will need to be created. The next step is to investigate what kinds and magnitudes of modifications are needed to allow installation of the new mounts onto the helicopter simulation seat shown in Figure 1, Chapter 1.

In summary, we believe the issue of helicopter seat vibrations warrants further investigation. Helicopters are relied on heavily in both military and civilian operations and the health of the pilots is of great importance. We see Fluidlastic^{TM} mounts as a compact and simple way to further reduce vibrations in a helicopter seat and improve pilot well-being.

REFERENCES

[1] **Griffin, M. J.** *Handbook of Human Vibration.* San Diego : Academic Press Inc., 1990.

[2] **Dupuis, H., Zerlett, G.** Whole-body vibration and disorders of the spine. *International Archives of Occupational and Environmental.* 1987, Vol. 59, pp. 323-336.

[3] *Backache in helicopter pilots [Abstract].* **Sliosberg, R.** Madrid, Spain : s.n., 1962. Translation of Reports and Communications of the 11th International Aeronautical and Cosmonautical Medical Congress. Library translation 1857. Abstract retrieved from Aerospace and High-Technology Database. N76-12700.

[4] *Lytic Spondylolitsthesis in Helicopter Pilots.* **Froom, M.D., P., et al.** s.l. : Aviation, Space, and Environmental Medicine, 1984, Vol. 55, pp. 556-557.

[5] *Low back pain.* **Devereaux, M.D., M.** 2, s.l. : The Medical Clinics of North America, 2009, Vol. 93, pp. 477-501. Retrieved from MD Consult database. 19272519.

[6] *Whole Body Vibration Exposure for MH-60S Pilots.* **Harrer, Kristin L., et al.** Salt Lake City : Proceedings of the Forty Third Annual SAFE Association Symposium, 2005.

[7] **Bongers, P. M., et al.** Back pain and exposure to whole body vibration in helicopter pilots. *Ergonomics.* 1990, Vol. 33, 8, pp. 1007-1026.

[8] **Paddan, G. S. and Griffin, M. J.** Effect of Seating on Exposures to Whole-Body Vibration in Vehicles. *Journal of Sound and Vibration.* 2002, Vol. 253, 1, pp. 215-241. Retrieved from Compendex.

[9] **Flannelly, William G.** *Dynamic Antiresonant Vibration Isolator. 3,322,379* United States of America, May 30, 1967.

[10] **Milko, Tim, Heilman, Paul and Wells, Stephen.** Sikorsky Vibration Simulation Seat. 2008. Final Report from Senior Design Project, Pennsylvania State University.

[11] *Development of adaptive helicopter seat systems for aircrew vibration.* **Chen, Yong, Wickramasinghe, Viresh and Zimcik, David G.** s.l. : Proceedings of SPIE - The International Society for Optical Engineering, v 6928, 2008. Active and Passive Smart Structures and Integrated Systems. Retrieved from Compendex. 0277786X.

[12] **Hiemenz, Gregory J., Hu, Wei and Wereley, Norman M.** Semi-Active Magnetorheological Helicopter Crew Seat. *Journal of Aircraft.* May/June, 2008, Vol. 45, 3, pp. 945-953. Retrieved from Compendex.

[13] **LORD Corporation.** LORD Industrial Parts Catalog. *LORD Corporation Web site.* [Online] August 2009. http://www.lordfulfillment.com/upload/PC7000.pdf.

[14] **Podesta, J. R.** *User's Guide to the Application of Fluidlastic(R) Mounts.* [Document] Erie, PA : LORD Corporation. Access through http://www.lord.com. LL7418.

[15] **LORD Corporation.** Fluid Vibration Isolation and Damping. *LORD Corporation.* [Online] 2008. [Cited: October 30, 2009.] http://www.lord.com.

[16] **Smith, Suzanne D.** The Effects of Prototype Helicopter Seat Cushion Concepts on Human Body Vibration Response. *Journal of Low Frequency Nois, Vibration and Active Control.* 1998, Vol. 17, 1. Reprinted by United States Air Force Research Laboratory, Report No. AFRL-HE-WP-SR-2001-0011.

[17] **United States. Federal Avaition Administration.** *Basic Helicopter Handbook.* 1995.

[18] **Gordon, Elmaree and Ahroon, William A.** *Noise Levels in the USAARL NUH-60 (Black Hawk) Aeromed Flight Simulator.* Fort Rucker : U. S. Army Aeromedical Research Laboratory, 2000. USAARL Report No. 2000-19.

[19] **Kulakowski, Bohdan T., Gardner, John F. and Shearer, J. Lowen.** *Dynamic Modeling and Control of Engineering Systems.* New York : Cambridge University Press, 2007.

APPENDIX A

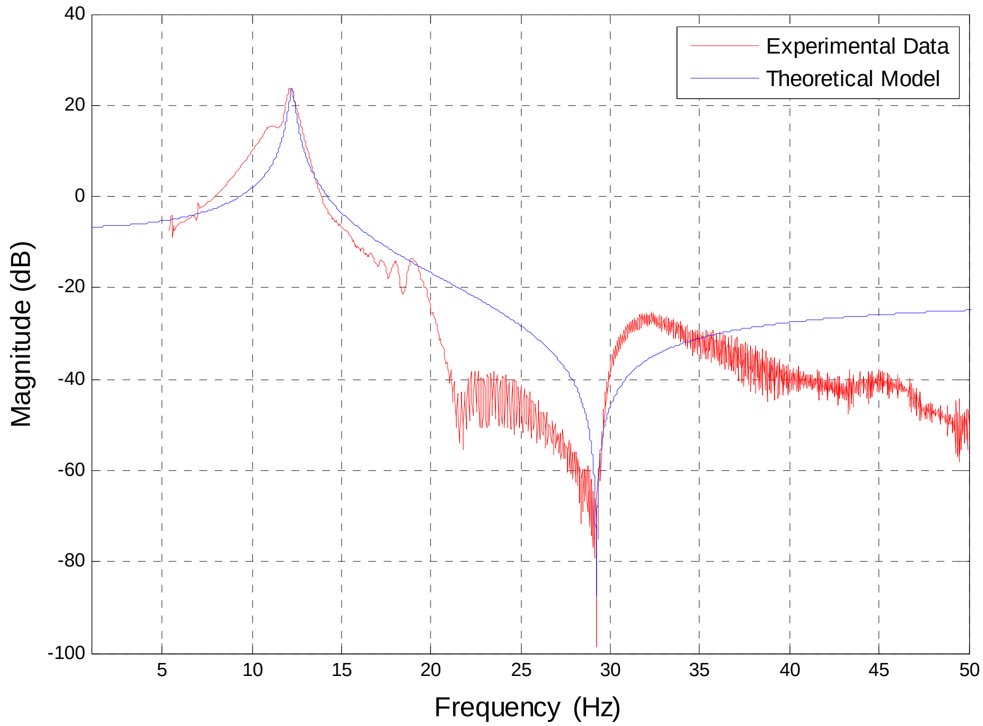

Figure 19: Theoretical and Experimental Frequency Response of Fluid Mount #1 (P = 229.5 lb_f)

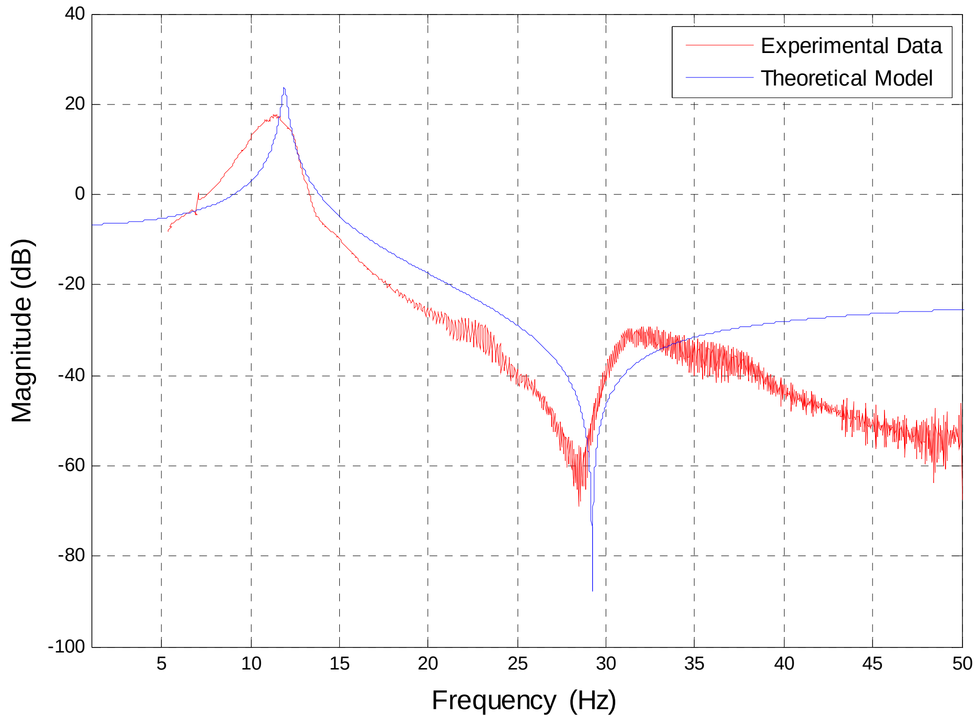

Figure 20: Theoretical and Experimental Frequency Response of Fluid Mount #1 (P = 249.5 lb_f)

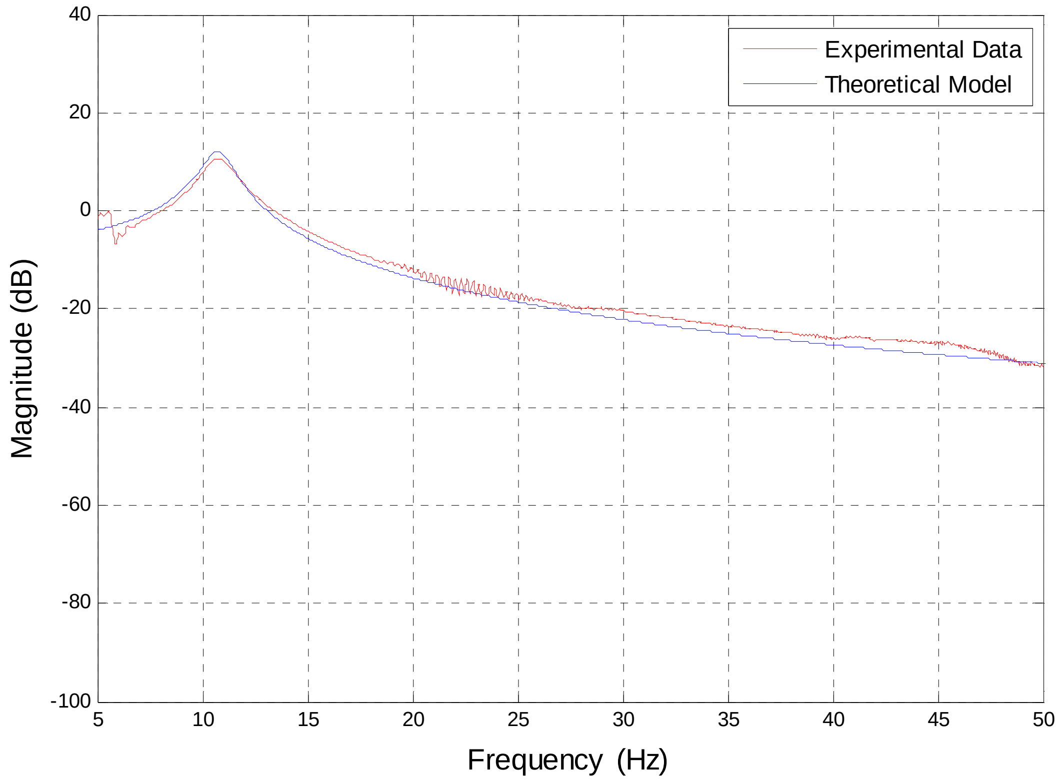

Figure 21: Theoretical and Experimental Frequency Response of Foam Cushion (P = 229.5 lb_f)

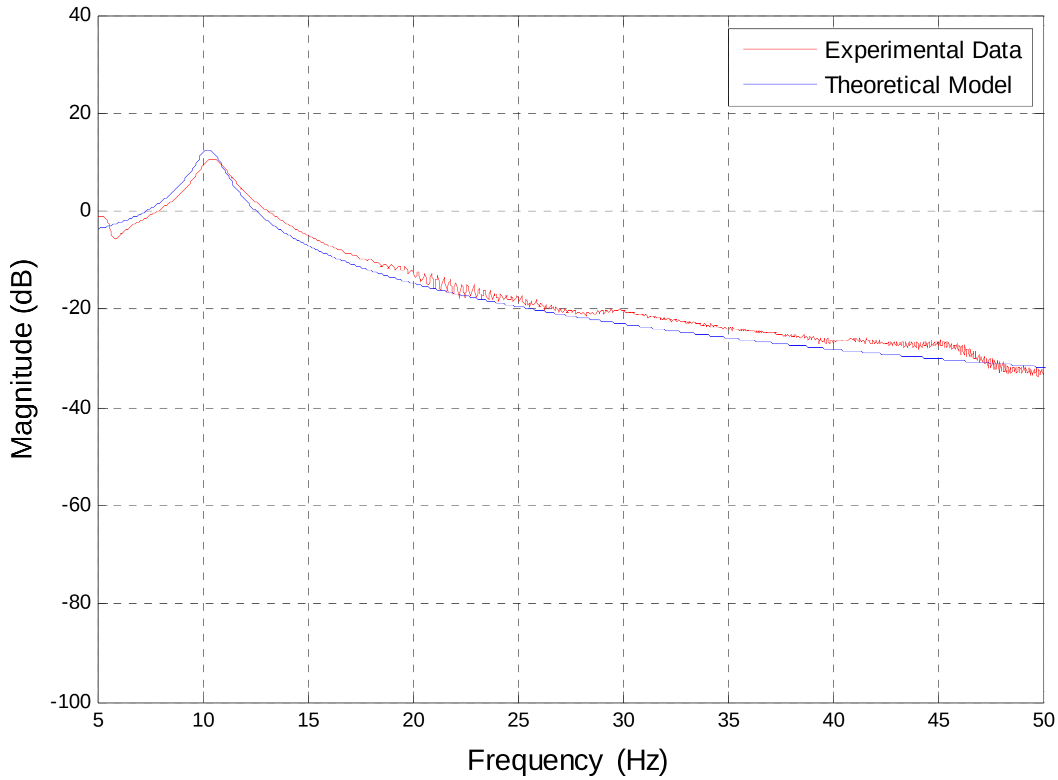

Figure 22: Theoretical and Experimental Frequency Response of Foam Cushion (P = 249.5 lb_f)

ACADEMIC VITA

Angela N. Santo
3042 Kenwick Circle
Bethlehem, PA 18017
ans184.asanto@gmail.com

EDUCATION: Bachelor of Science Degree in Mechanical Engineering
Penn State University, Fall 2009
Honors in Mechanical Engineering
Thesis Title: Performance of Industrial Fluidlastic^{TM} Mounts and Feasibility for Helicopter Seat Application
Thesis Supervisor: Christopher D. Rahn

EXPERIENCE: Co-op, LORD Corporation

- Employed in design engineering group and manufacturing plant at vibration and motion control company.
- Designed, analyzed and tested elastomeric vibration control products for helicopters.
- Completed instructional documentation and lean manufacturing projects in silicone product manufacturing area for various aircraft parts.

Supervisors: Peter Jones, Megan Agrafiotis
Spring/Summer 2008, Summer 2009

Intern, Minrad International, Inc.

- Developed solutions to various packaging issues at pharmaceutical manufacturing plant.

Supervisor: Jeff Drake
Summer 2007

AWARDS: Dean's List
Phi Eta Sigma Honor Society
H. Thomas and Dorothy Willits Hallowell Scholars Endowment
Paul Morrow Endowed Scholarship
Louis A. Harding Memorial Scholarship

ACTIVITIES: Society of Women Engineers
American Society of Mechanical Engineers
American Helicopter Society
Penn State Dance Marathon, Rules and Regulations Committee
Pride of the Lions Basketball Pep Band